The aerodynamic performance of a range of FIFA approved footballs.

Martin Passmore[1], David Rogers[1], Simon Tuplin[1], Andy Harland[1], Tim Lucas[2], Chris Holmes[2]

Abstract

Much discussion surrounds the flight of a football especially that perceived as irregular and is typically done so with little understanding of the aerodynamic effects or substantive evidence of the path taken. This work establishes that for a range of FIFA approved balls there is a significant variation in aerodynamic performance.

This paper describes the methods used for mounting stationary and spinning footballs in a wind tunnel enabling accurate force data to be obtained, and the analysis techniques used. The approach has been to investigate a number of scenarios: Non-spinning Reynolds Sweep, Unsteady Loads, Orientation Sensitivity (Yaw Sweep) and Spinning Reynolds Sweep. The techniques are applied to a number of footballs with differing constructions and the results reported. To put the aerodynamic data into context the results are applied in a flight model to predict the potential differences in the behaviour of each ball in the air.

The paper concludes that although the drag characteristics are different for the different balls tested the simulation suggests that this has only a limited effect on the flight of the ball. It is also shown that the unsteadiness of the aerodynamic loads is unlikely to be responsible for unpredictable behaviour. However, it is also shown that there are significant differences in the lateral aerodynamic forces for a range of FIFA approved match balls, and that these aerodynamic differences have a significant effect on the flight path for both spinning and for slowly rotating balls.

Keywords

Football, aerodynamics, free flight, Magnus force, spinning, orientation sensitivity.

1. Introduction

Football is a truly global sport, enjoyed in virtually every country across the globe. The Fédération Internationale de Football Association (FIFA) World Cup™, that takes place every four years, is considered the pinnacle of the sport with games broadcast to over 200 countries and the final match attracting an audience of around 700 million viewers.

A feature of the World Cup™ over the last 30 years has been the use of a new football, launched in the run up to the competition. Since 1997 FIFA have provided clear guidelines for the manufacture, quality and dynamic response of match footballs (1). For example the weight must be 410 – 450g and the circumference 680 – 700 mm, there are also requirements regarding the sphericity, loss of pressure, water absorption, coefficient of restitution and shape and size retention.

There is no equivalent standard for the aerodynamic response of the ball and this study was undertaken to provide a summary of the aerodynamic performance for a range of designs that meet the current guidelines. This paper describes the methods used to assess the aerodynamic performance of the FIFA approved balls. The experimental approach used to gather the aerodynamic data is described and the main results for the balls are summarised alongside a smooth sphere to put these results in context. In practice the raw aerodynamic data generated from the experimental work does not reveal how individual balls perform in flight, so the aerodynamic data is also analysed via a flight prediction model and the flight data used to illustrate and characterise the performance of the balls.

2. Background

The focus of the aerodynamic performance is on the period of free flight after the ball has been struck and before it comes into contact with the ground. During the free flight period it is assumed that the ball has recovered from the initial impact and an aerodynamic force acts upon the ball that can be separated into a drag component in line with the direction of motion and a force perpendicular to the direction of travel and where relevant also perpendicular to the spin axis. The forces are a consequence of the imbalance in the surface pressure distribution and surface shear stress distribution. In practice with a bluff -body, such as a football, the forces are dominated by the surface pressures and the non-uniform distribution can result from several different mechanisms. In addition it is noted that the aerodynamic force generates a small moment about the ball centre.

Experimental work by Achenbach (3,4,5) in the early 1970's established widely used benchmark data for the generic non-rotating sphere. Achenbach used a 200 mm diameter polished aluminium sphere and tested over the Reynolds number range of $5x10^4$ to $6x10^6$. Typical results are illustrated in Figure 1.

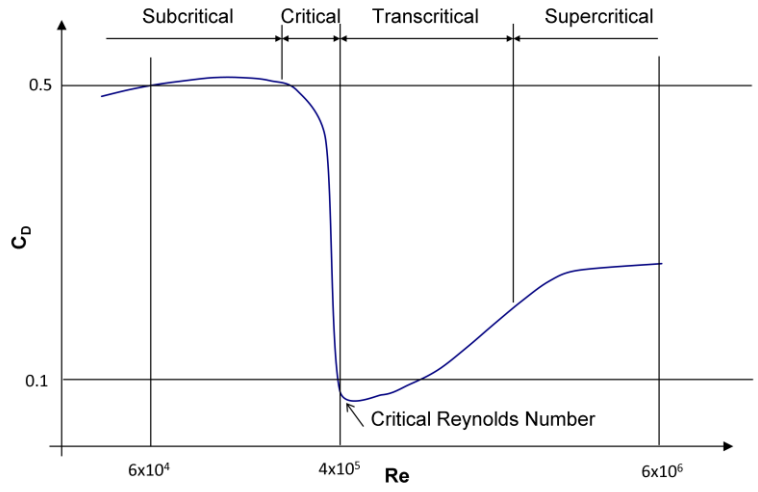

Figure 1 Smooth sphere: C_D against Reynolds number.

In the sub-critical region C_D is approximately independent of Reynolds number. In this regime the laminar separation, occurring at approximately 82° from the stagnation point, produces a large wake and the lack of pressure recovery gives a high drag coefficient. In the critical region the separation point moves rapidly downstream to approximately 120° with transition occurring first in the free shear layer associated with an intermediate separation bubble and then immediately without the formation of the bubble where the drag coefficient then reaches a minimum at a Reynolds number of approximately 4×10^5. In the supercritical region following this, transition occurs at approximately 95° and the drag coefficient increases as the position of separation moves and the skin friction contribution varies. At Reynolds numbers above 1.5×10^6 an approximately constant C_D is again seen as transition moves to the forward part of the sphere. Achenbach (3) also investigated the effect of surface roughness using spheres with five different surface roughness values and observed that for increasing roughness the critical Reynolds number decreases, and both the minimum drag value and the trans-critical drag coefficient increase. An additional feature of all bodies of this type, where the wake is large and dominates the aerodynamic drag is relatively high levels of unsteadiness. This may lead in some cases to significant unsteady loads.

For a spinning ball that arises when the ball is deliberately struck off centre the effect of the rotation is to advance the separation point on the counter rotating side, and to delay it on the opposite side. This generates an imbalance in the pressure and results in a lateral deflection in the flight of the ball in the direction of the lowest pressure region. This is generally known as the Magnus effect. Given that the player deliberately applies the spin to the ball and the ball will then fly in the same manner every time,

this is a predictable effect, however Passmore (2) shows that the degree of swerve in the ball may differ depending on the ball design.

Asymmetric flow fields may also be generated as a consequence of an asymmetric ball or panel arrangement; Passmore (2) shows that ball orientation in a non-spinning case can produce significant lateral forces. These forces are similar to those occurring in the knuckle ball in Baseball, where the pitcher throws the ball with little or no spin in order to achieve an unpredictable flight. In football it is difficult to strike the ball with little or no spin so such effects are unlikely to be under the control of all but the very best players, for others this may therefore be considered to be unpredictable. In practice though if we know the forces that are generated and the initial conditions, including orientation and spin rate, then the flight is entirely predictable.

As it is not clear which of the mechanisms described above might be responsible for unpredictable behaviour in practical play and given that much of the description of unpredictable behaviour is not supported with measurements, the approach here has been to investigate a number of scenarios.

- Static Reynolds sweep (Non-spinning)
- Unsteady loads
- Orientation sensitivity (Low Spin Effects)
- Spinning tests (Spinning Reynolds Sweep)

The data that is generated is then supported with detailed flight modelling. This provides context to the measurements and allows comparisons between balls.

3. Experimental method

The open circuit wind tunnel employed in this work has a closed working section of 1.32x1.9m and a maximum air speed of 45 ms^{-1}. For the work reported here the upper test speed is limited to 30 ms^{-1} more in line with the maximum of 34ms^{-1} reported by Neilson (7). A speed of 30 ms^{-1} equates to a diameter based Reynolds numbers of Re = 4.5 $x10^5$. The working section turbulence intensity is approximately 0.2% and spatial uniformity ±0.2% of mean velocity, the tunnel blockage is 1.7%. For further details of the tunnel, see Johl (8).

The aerodynamic balance is a high accuracy 6-axis under-floor virtual centre balance designed for aeronautical and automotive testing. The quoted accuracy for the relevant balance components is ± 0.012N for drag and ± 0.021N for side force and based on the maximum forces from a football at maximum spin rate and tunnel speed, the resolution obtainable is approximately; ± 0.05% of the maximum force for drag and ± 0.50% of the maximum force for the lateral component.

Raw data is resolved into wind axis and the drag and lateral force coefficients calculated from the equations below. Given the very low blockage ratio the coefficients do not have a correction applied.

$$C_D = \frac{D}{\frac{1}{2}\rho A v^2} \qquad C_{lat} = \frac{F_{lat}}{\frac{1}{2}\rho A v^2} \quad [1]$$

The Magnus force associated with ball aerodynamics can operate in any direction; it is dependent on the spin axis orientation. Hence the term lateral force is used rather than lift or side as it will be the force normal to the drag component, rather than force acting in a prescribed direction.

3.1 Ball mounting

Two methods of mounting the ball in the tunnel are employed. The first uses the approach described by Passmore (2) using a single shaft from below, figure 2a.

Figure 2a Below Mount; 2b Rear Mount of a ball in the wind tunnel.

This approach is the practical solution when the ball must be spun while mounted to the balance, or when the orientation effects are measured. In this case a shaft diameter of 20mm ensures that the shaft does not deflect significantly under load (<0.5mm) whilst also being less than the recommended 10% of the ball diameter (6,4). The authors have tested with smaller diameter shafts and found that down to 10mm diameter there is little change in the measured lateral forces. It is also not possible to spin the ball on diameters less than 20mm as the increased amplitude of precession will strengthen any out of balance, potentially leading to failure of the system and damage to the balance. The second method mounts the ball on the same 20mm diameter shaft but from a rear mounted cantilever such that the support comes through the wake of the ball, see figure 2b. This approach allows for a more representative measurement of the aerodynamic drag. To account for the presence of the support in each case a tare test is conducted in which the direct support and support interference effects are measured with the ball mounted in its usual location but independently of the support structure. This tare can then be subtracted to yield the isolated ball forces. In both orientations the footballs are mounted to the shaft by filling them with a two-part poly-urethane expandable foam; to ensure sphericity this is carried out with the ball in a production mould. When cured the ball is drilled to accommodate the shaft. The method is described in more detail by Passmore (2).

3.2 Spinning facility

The ball spin apparatus described by Passmore (2) is shown mounted on the balance under the tunnel working section in Figure 3. The structure seen in the figure supports a bearing casing and motor driving the ball support shaft that protrudes through the tunnel floor. In the work reported by Passmore(2), using the same facility, repeatability tests showed a maximum scatter of approximately ±0.1N on both drag and lateral force at the 95% confidence level. This translates to an error in the drag and lateral force coefficients of ±0.04 at $10ms^{-1}$, ±0.009 at $20ms^{-1}$ and ±0.005 at $30ms^{-1}$.

Figure 3 Spin rig: View from under working section floor.

3.3 Ball types.

6 ball types are analysed in the results sections that follow. These include the 2006 and 2010 World Cup™ balls; two balls currently used in National leagues, a FIFA inspected ball and a prototype with a much simplified surface panel arrangement. Note that all the balls are of the same diameter as they were filled in the same production mould. In addition a rapid prototype smooth sphere is included. The identification of the balls is summarised in Table 1. Direct reference to individual balls is deliberately avoided so that the analysis can focus on actual performance rather than preconceptions of the expected performance.

Ball Identification	Status	Ball Diameter (mm)
BALL 1	FIFA Approved, Match Ball	216
BALL 2	FIFA Approved, Match Ball	216
BALL 3	FIFA Approved, Match Ball	216
BALL 4	FIFA Approved, Match Ball	216
BALL 5	FIFA Inspected	216
BALL 6	BALL1 Prototype; reduced surface features	216
-	Smooth sphere. (Rapid prototype)	220

Table 1 Summary of ball types

3.4 Test Matrix

Table 2 is a summary of the tests undertaken for each of the balls. Experiments where a single ball is used are detailed in the relevant sections.

Test Type	Nominal Wind speed [m/s]	Spin Rate [Rpm]	Mounting Orientation
Reynolds Sweep	7.5 10 11 12 13 14 15 16 18 20 25 30 35	0	Behind
Yaw Sweep	30	0	Below
Spin	30	100 200 300 400 500	Below

Table 2 Summary of test types

4. Flight model and its application

The flight model is based on that reported by Bray (10) and used in Passmore (2). For simplicity the spin axis is assumed vertical. The model is implemented using first order backward differencing, where the time step has been reduced until there is no significant change in the calculated flight path. The drag and lateral force coefficients are obtained from an interpolation of the wind tunnel data for the particular ball type. In the quasi-static low spin analysis the look up table contains data for the relevant coefficient against orientation angle and for the spinning tests a two dimensional interpolation of ball speed and ball spin speed is required.

The flight model can be used to predict a single flight for a particular set of initial conditions or used to generate a range of kicks with different initial conditions that can then be used to characterise the overall performance of the ball. This latter approach is particularly important when considering orientation effects because the trajectory is strongly dependent on the initial conditions.

5. Results and analysis

5.1 Reynolds sweep and drag

Results are shown for drag coefficient against Reynolds number in Figure 4; the data were obtained with the rear mounted support. For comparison the results from Achenbach (3) are included and compared with the smooth sphere of the same diameter as a football. The results for this sphere match those of Achenbach well and provide confidence in the method and experimental technique.

All six footballs show a broadly similar overall characteristic but there are some differences through transition and in the post critical drag. The sub-critical drag coefficients are similar for the six balls and at these low Reynolds number the aerodynamic loads are sufficiently small that they have a limited effect on the flight.

BALL 6 has the lowest post critical drag and is significantly lower than BALL 4 at approximately half. The significance of these differences in post-critical drag can be assessed using a single typical kick from 25 metres from goal with an initial speed of 30m/s, see Table 2. For balls 1 to 6 the average flight time is 0.97s, but all balls are covered by a range of only ±30msec. This is not considered important in the context of the game. It is worth noting that despite a much lower post-critical drag the smooth sphere has an overall flight time similar to that of BALL 6. This is because transition for the smooth sphere is at a much higher Reynolds number and for the 30m/s kick the ball passes though transition. The consequence for the real balls is that because transition is at a relatively low Reynolds number only low speed kicks actually operate in this regime and under these the aerodynamic loads are insufficient to make a significant impact.

BALL Identification	Time to Goal [s]	End Velocity [ms^{-1}]
1	0.98	23.0
2	0.96	23.9
3	0.95	24.4
4	1.00	22.3
5	0.99	22.8
6	0.94	24.9
Smooth Sphere	0.93	24.9

Table 3 Assessment of the Influence of Reynolds Data on a Free Kick

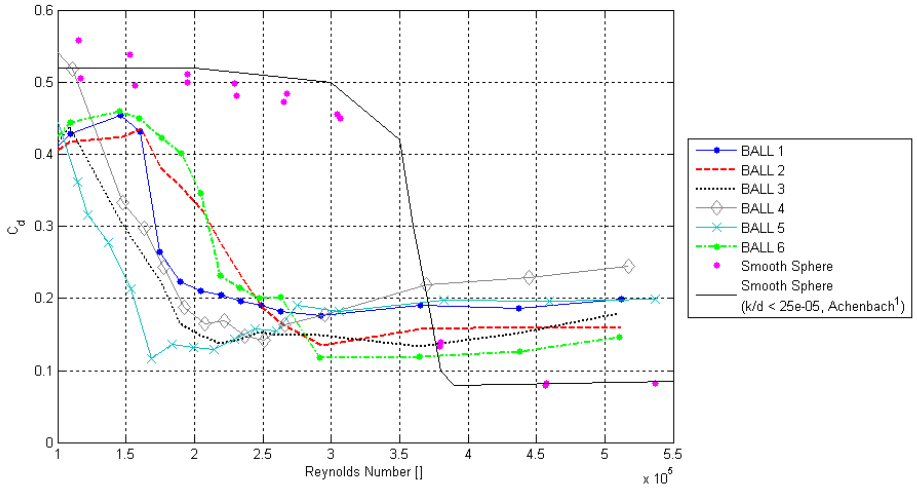

Figure 4 Drag coefficients against Reynolds number

As the remainder of the tests reported in the later sections all employ the mounting support from below rather than from behind, a straight comparison of the two methods is given in Figure 5. Both cases are corrected for direct support and support interference effects. The higher overall drag coefficient for the mounting from below arises because the support causes a localised separation that feeds into the wake and reduces the pressure.

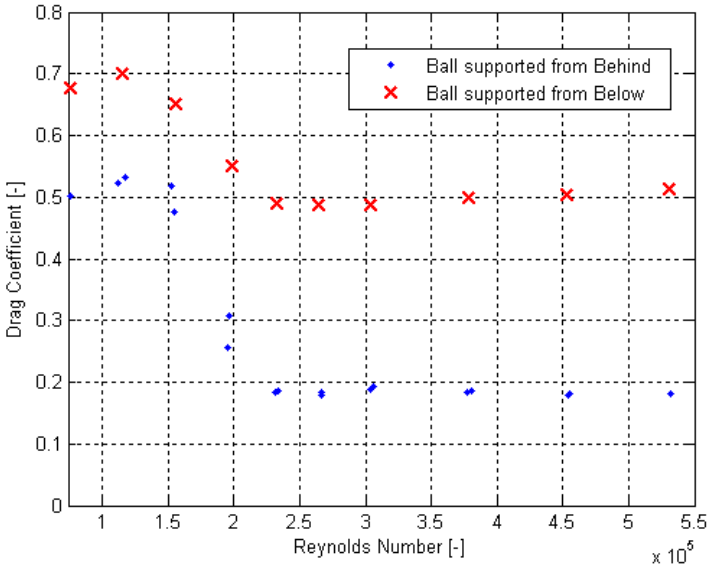

Figure 5 Comparison of mounting method on Reynolds data

In the lateral measurements that follow, the ball is necessarily mounted from below using a 20mm shaft. It is recognised that the results for the drag coefficient above may be to some degree impact on the lateral forces, but will have the same influence for all balls. This however highlights the need in future work to specifically assess these effects and the need to generate high quality real flight validation data so that the complete wind tunnel and simulation technique can be more fully evaluated.

5.2 Unsteady forces.

The under-floor balance installation used throughout the measurements described in this paper has the capability to record dynamic forces (up to 300Hz) as well as time averaged results and can therefore be used to determine the unsteady forces that arise as a consequence of the turbulent wake associated with the football. In practice the balance used to measure the loads has a natural frequency at 5Hz so based on an inspection of the measured power spectral density the data is filtered in the frequency domain using a low pass filter with a cut off at 4Hz. A sample set of data is shown in Figure 6.

The unsteady measurement was repeated at a number of tunnel speeds and the RMS calculated. To assess the impact of the fluctuating forces on the ball flight the RMS component is superimposed onto an otherwise steady lateral force and the flight paths compared. The maximum differences in path for a 45metre long flight are ±5mm. This result is true of both spinning and non-spinning cases.

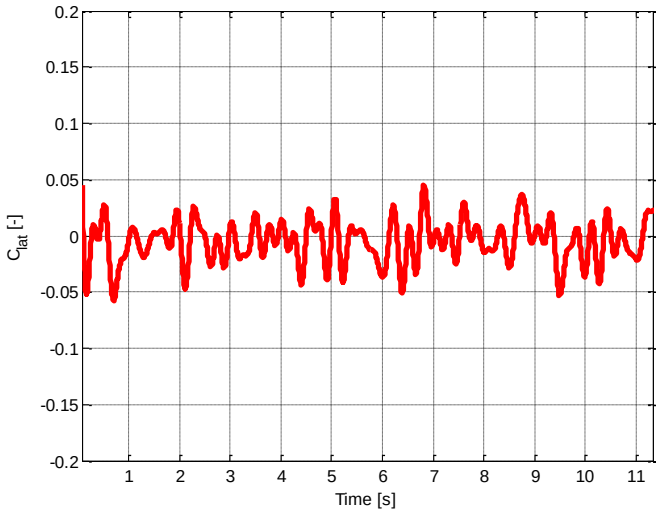

Figure 6 Unsteady lateral forces on BALL 1

5.3 Quasi-Static low spin rate effects

The effects of low spin rates on the flight of the ball are explored by measuring the orientation sensitivity of the ball as this makes it possible to determine any lateral movement due to assymetry. Figure 7 shows the orientation sensitivity for each of the six balls, in each case the data was acquired at 30m/s and with the ball mounted from below the balance is rotated from -145 to +145 degrees in 5 degree increments. BALL2 data was acquried before a full sweep was availible, hence data presented for -90 to +90 degrees. At each point a 20 second average is obtained for each force component. The results are corrected for wind off balance tare and wind on support and support interference and resolved into wind axis.

While it is clear that there are differences between the balls and that they are all to some degree sensitive to orientation it is difficult from the raw aerodynamic data to draw conclusions regarding the actual performance in flight. For example, to assess the quasi-static low spin performance it is necessary to account for both the amplitude of the variation in lateral coefficient and the number of cycles (the repetition wavelength) that occur as the forces fluctuate between positive and negative. To investigate this, simulated wind tunnel data was generated with varying amplitude and repetition frequency. An example is shown in Figure 8 where the repetition wavelength is 180 degrees and the amplitude 0.1.

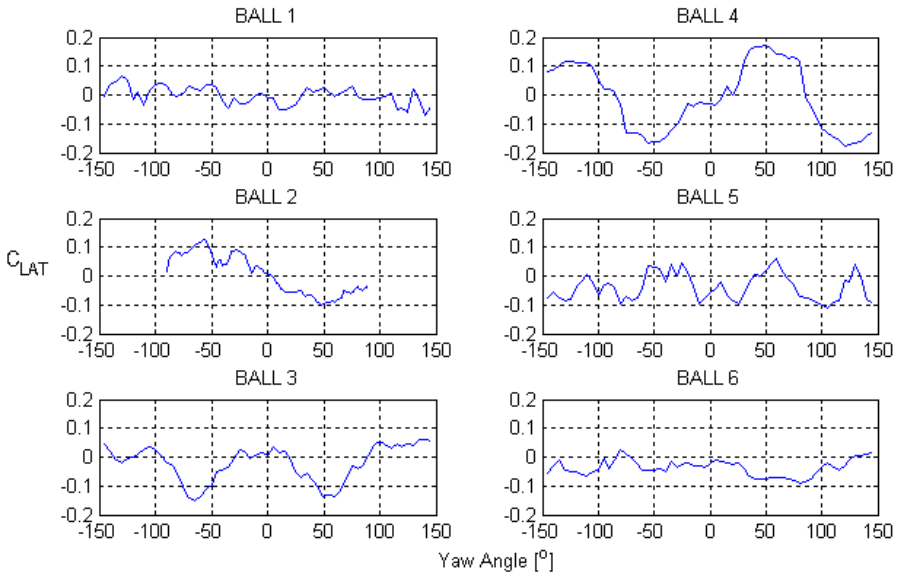

Figure 7 Orientation sensitivity of tested balls

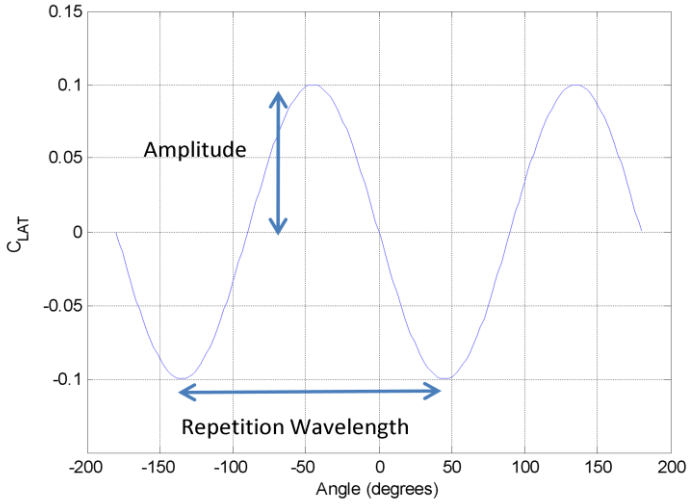

Figure 8 Example simulated lateral force coefficient

Using the simulated wind tunnel data as input to the flight model the effects of amplitude and frequency were determined by performing 500 kick simulations with a range of ball start orientations varying from -180° to + 180° in 15° steps and ball rotational speeds varying from 0rpm to 10rpm. From each kick the RMS deviation from its initial flight trajectory is calculated and averaged over the 500 kicks to synthesise a ball characterisation parameter for quasi-static conditions. The lower the overall RMS deviation the less in flight deviation due to flow asymmetry expected. The results of the study are summarised in Figure 9 which shows that the RMS deviation is reduced with reducing repetition wavelength and increased with increasing amplitude. It is noted though that while the lowest deviation would be achieved by reducing both the magnitude of the lateral coefficient and the repetition wavelength, it is possible to achieve similar overall deviation through a number of combinations. The RMS deviation calculated from the 500 simulated quasi-static kicks is therefore a useful parameter for differentiating between real balls performance.

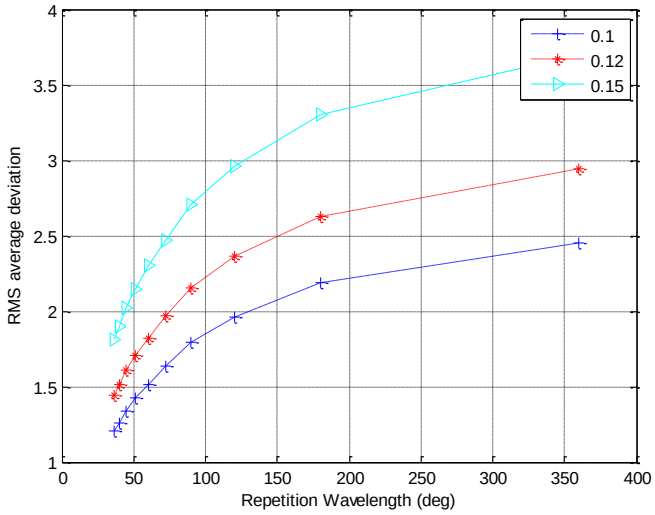

Figure 9 Effect of lateral force coefficient repetition frequency and amplitude on RMS deviation.

Applying the technique to the real ball data shown in Figure 7, the synthesised RMS deviation is summarised for the six test balls in Figure 10. The improvement of BALL 1 over the BALL 4 is clearly evident and consistent with the results in Figure 7, BALL 4 is shown to exhibit relative high lateral force coefficients combined with a high repetition wavelength and BALL 1 has a low amplitude and low repetition wavelength. It is also worth noting the significant increase in RMS that occurs when the surface features are reduced from BALL 1 compared to BALL 6. Removing these increases the amplitude of the lateral forces and the repetition wavelength and produces a ball with increased variability during flight. The other balls all have a differing RMS response which correlates with their yaw response.

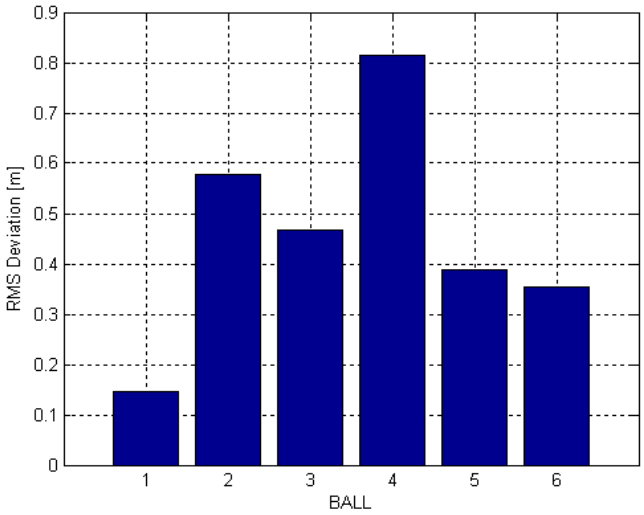

Figure 10 Ball orientation sensitivity - RMS deviation

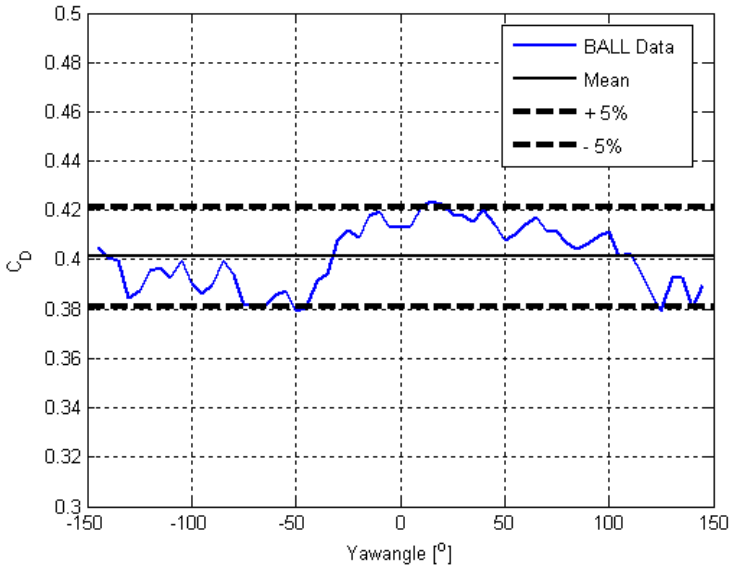

Figure 11 Sensitivity of drag coefficient to ball orientation

While conducting the lateral force sensitivity experiments the ball drag coefficient was also extracted; while it is noted that this orientation gives a high overall drag coefficient because the mounting is from below, it is useful to note as in Figure 11, a typical example, that for all balls there is an orientation dependent variation in the drag coefficient of order ±5% from the mean. The variation arises out of the same flow mechanisms that generate the lateral forces and suggest that reporting and comparing the drag coefficients of a number of balls tested in a single arbitrary orientation is not useful and that any conclusions drawn from this regarding the flight of the ball are unlikely to be substantiated. In the Reynolds sensitivity data presented in Figure 4, every ball was tested in a zero degree configuration that gave a symmetrical panel arrangement and zero lateral force.

5.4 Spin effects

The spin technique described by Passmore (2) is used to generate the data for BALL 1. The results are shown in Figure 12 using the usual method of plotting lateral coefficient against the non-dimensional spin ratio ($\omega r/U$). Each curve is a fixed Reynolds number, so increasing spin ratio implies an increase in the angular velocity. For all Reynolds numbers the lateral coefficients that can be generated are much greater than those experienced due to orientation sensitivity, where for this particular ball they are restricted to approximately ±0.05 (Figure 7). It is also worth noting the reverse in direction of the lateral force that occurs for the three lowest Reynolds numbers at low spin ratios.

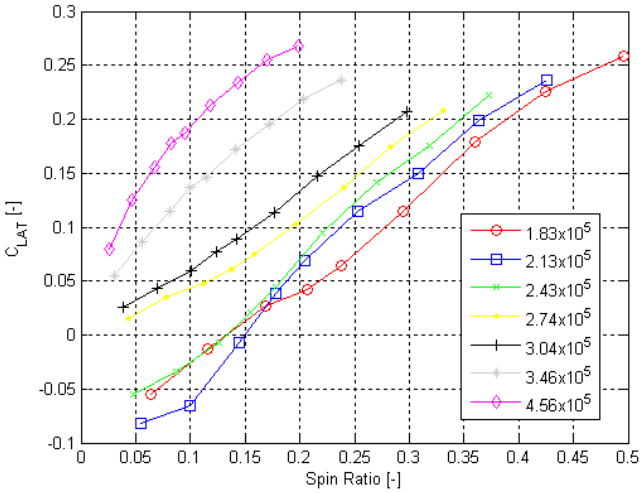

Figure 12 Lateral coefficients against spin ratio for fixed Reynolds number.

It is also worth noting that while it is possible to generate quite large lateral coefficients at the lower Reynolds numbers shown in the figure, they require high spin rates. For example at the lowest Reynolds number shown a spin ratio of 0.4 generates a lateral coefficient of 0.2 but requires a spin rate of approximately 400rpm. It is also of note that the lowest spin ratios at each Reynolds number represent spin rates of approximately 70rpm and the Magnus effects are still significant. This is contrary to the assumption by Carre (9) for the flight simulation that is reported. The data presented does not collapse onto a single curve so the Magnus force is not solely dependent on spin ratio, but rather is also strongly Reynolds dependent.

The methods used to derive the data in Figure 12 were based on those reported by Passmore (2), where the ball is tested across a matrix of fixed wind and spin speeds. This is very time consuming to perform and analyse so the spin method has been modified to improve productivity by running at a fixed spin speed while the tunnel speed is reduced from a maximum of 30 ms^{-1} down to 10 ms^{-1}. Data is sampled continuously throughout the dynamic test which can then be repeated at a different spin speed. Results are presented for two spin speeds, 100rpm and 500rpm, in Figure 13. The results are presented using Reynolds number rather than spin ratio as in this case it makes the presentation a great deal clearer. The range of Reynolds numbers is representative of a game situation.

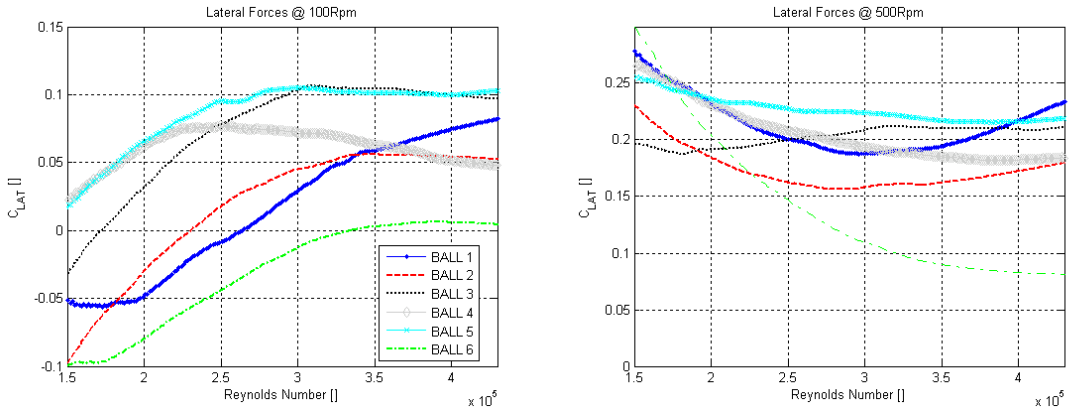

Figure 13 Comparison of lateral forces for spinning balls

At 500rpm all the balls produce significant levels of Magnus force. BALL 6 produces an unusual response for a football, and is thought to arise because it is much closer to a smooth sphere than to a conventional football. This is an important result because this ball produced a relatively low RMS deviation in Figure 10. At 100rpm the balls all produce a similar trend but with significantly different actual levels of Magnus effect. BALL 5 produces the largest lateral coefficient and it is positive apart from at the lowest speeds tested, i.e. it is a conventional Magnus effect. Both BALL 1 and BALL 2 show a degree of reverse Magnus at the lower Reynolds numbers. In these circumstances the ball will either swerve in the opposite direction to conventional Magnus or, given the low Reynolds numbers that this occurs at, where the forces are relatively low, it may fly much straighter than other balls. BALL 6 produces a reverse Magnus effect throughout much of the range tested, given that this ball design demonstrates relatively good characteristics under quasi-static conditions this highlights the need to consider a number of aspects of the performance in the final design. It can be surmised from this that it is the general roughness of the surface that is required to generated sufficient circulation to instigate the associated Magnus force.

Figure 14 summaries the effect of the lateral forces under spinning conditions on the flight of the ball. Here a single kick is simulated because the initial orientation is not important. The RMS deviation of the flight is again used to determine the degree of lateral movement and is plotted against the initial spin rate.

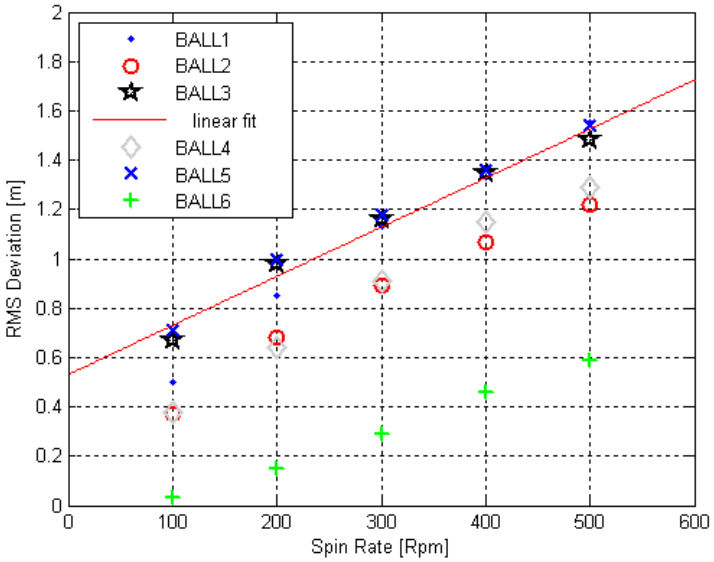

Figure 14 Significance of Magnus force on flight deviation

Figure 14 shows that there is significant variation between the balls. A player who uses different designs of ball from one match to the next, or indeed trains with a different ball would need to adapt to the changes in performance. Comparing the balls directly the ordering of magnitudes of RMS deviation of the balls is identical to that of the post-critical Reynolds number that can be extracted from figure 4. The latter is known to be directly influenced by surface roughness and suggests that it is this general surface roughness that generates the circulation around the ball and hence the lateral force. Placing a trend line through the data (BALL 3 used as an example and a linear fit is used as Kutta-Zhukovskii theorem suggests lateral force is proportional to spin rate) produces an interesting result. It would be expected that at zero spin there would be zero deviation, yet the fit demonstrates otherwise. It cannot be true that zero circulation produces a lateral force and this result confirms the earlier work that the orientation is the overarching factor on the flow at very low spin rates. Further work is necessary to clearly identify the cross-over point between the two mechanisms.

6. Conclusions

- A comprehensive study of the aerodynamic performance of a range of FIFA approved footballs has been conducted, including Reynolds sensitivity effects, low spin rate orientation (knuckle) effects, unsteady aerodynamic loads and Magnus effects.
- The experimental data acquired in the wind tunnel is used in a flight model to simulate the predicted flight arising as a consequence of the aerodynamic loads.
- All balls tested showed similar characteristics with Reynolds number but with some differences through transition and quite large differences in the post critical drag. However these differences in post critical drag were shown to have only a limited effect on the flight of the ball. For a kick with an initial velocity of 30m/s the average flight time for the six balls, over a distance of 25m is 0.97 s ±30 ms.
- The unsteady aerodynamic loads were measured and are shown to have a negligible effect on the ball trajectory.
- Orientation data was collected for each ball and overall RMS deviation derived from a simulated series of quasi-static low spin kicks is used to characterise the performance.
- The orientation tests show considerable differences in the RMS deviation for the six balls tested.
- The balls tested exhibit a range of different characteristics during spinning tests. All of the tested FIFA approved balls exhibit strong Magnus effects at high spin rates.
- Data at lower spin rates (100rpm) also show a range of responses between the ball types. All show some reverse Magnus effects though the onset of the reverse characteristic occurs at higher Reynolds numbers for some balls.
- Tests of a simplified ball that has a reduced amount of surface features shows relatively low orientation sensitivity but the same ball also generates small Magnus forces and a large amount of reverse Magnus.
- The data suggests that the orientation sensitivity effects and spinning effects are both influenced by the surface features on a ball but different flow mechanisms operate for the two cases. Further work is necessary to clearly identify the cross-over point between the two mechanisms.
- There is a pressing need for the generation of high quality real flight validation data to accurately quantify the effects of supporting a ball in a windtunnel.

7. References

1. http://fr.fifa.com/mm/document/afdeveloping/pitchequip/ims_sales_doc_05_2006_13411.pdf 'Testing and Certification for Footballs IMS: International Matchball Standard' FIFA, 2011. Viewed @ 10/05/2011.
2. Passmore, M.A., Tuplin, S., Spencer, A., Jones, R. Experimental studies of the aerodynamics of spinning and stationary footballs, *Proc. IMechE Part C J. Mechanical Engineering Science*, Volume 222 (C2), pp 207-211, 2008
3. Achenbach, E., The effects of surface roughness and tunnel blockage on the flow past spheres, *Journal of Fluid Mechanics*, V65(1) pp113-125, 1974
4. Achenbach, E., Experiments on the flow past spheres at very high Reynolds numbers, *Journal of Fluid Mechanics*, V54(3) pp565-575, 1972
5. Achenbach, E., Vortex Shedding from Spheres, *Journal of Fluid Mechanics*, V62 (2) pp209-221, 1974.

6. Watts, R.G., Ferrer, R., The lateral force on a spinning sphere: Aerodynamics of a curveball, *American Journal of Physics*, V55 (1) pp40-44, 1987.

7. Neilson, P.J., Jones, R. An exact method for the sphericity measurement of soccer balls, *Proceedings of the Institution of Mechanical Engineers, Part B: Journal of Engineering Manufacturing*, V217 (B5), pp715 – 719, 2003.

8. Johl, G., Passmore, M.A., Render, P., The Design Methodology and Performance of an Indraft Wind Tunnel, The Aeronautical Journal, 108 (1087), pp. 465-473 2004.

9. Carre, M.J., Goodwill, S.R., Haake, S.J., Understanding the Effect of Seams on the Aerodynamics of an Association Football, *Proc. IMechE Part C Journal of Mechanical Engineering Science*, Vol 219, 657 – 666, 2005.

10. Bray K, Kerwin D. G, Modelling the flight of a soccer ball in a direct free kick. Journal of Sports Sciences, vol 21, pp 75-85, 2003.

8. Acknowledgements

The authors would like to acknowledge the significant efforts made by the chief wind tunnel technician Rob Hunter.